Synthesis of zerovalent iron from water treatment residue as a conjugate with kaolin and its application for vanadium removal.

Adedayo Bello[a], Tiina Leiviskä[a]*, Ruichi Zhang[a], Juha Tanskanen[a], Paulina Maziarz[b], Jakub Matusik[b], Amit Bhatnagar[c]

[a]University of Oulu, Chemical Process Engineering, P.O. Box 4300, FIN-90014 University of Oulu, Oulu, Finland

[b]AGH University of Science and Technology; Faculty of Geology, Geophysics and Environmental, Protection; Department of Mineralogy, Petrography and Geochemistry, al. Mickiewicza 30, 30-059 Krakow, Poland

[c]Department of Environmental and Biological Sciences, University of Eastern Finland, FI-70211, Kuopio, Finland

*Corresponding author: tiina.leiviska@oulu.fi

ABSTRACT

This study was aimed at examining the possible utilization of iron-rich groundwater treatment sludge in the synthesis of zerovalent iron (ZVI) as a conjugate with kaolin clay (Slu-KZVI) and its use for vanadium adsorption from aqueous solutions. Iron was extracted from the sludge using 1 M HCl and was used in the ZVI synthesis by the sodium borohydride reduction method. The characteristics and performance of Slu-KZVI were compared to a synthetic iron ($FeCl_3 \cdot 6H_2O$) modified kaolin (Syn-KZVI). Adsorption results showed competitive performance between the two classes of KZVI with the Syn-KZVI slightly outperforming the Slu-KZVI. X-ray photoelectron spectroscopy and X-ray diffraction confirmed the formation of Fe^0 on the core-shell of both modified adsorbents. The surface analysis of Slu-KZVI additionally indicated the presence of P and Ca to a small extent, which originated from the sludge. Transmission electron microscopy (TEM) and Brunauer, Emmett and Teller (BET) characterization revealed similar morphology and particle size distributions. Both

classes of sorbents performed better in solutions with acidic and neutral pH (3-7), while the time required for optimal vanadium removal was 30 min. Surface complexation was probably the primary mechanism whereas simultaneous V(V) reduction and Fe oxidation (redox) reactions may also have taken place to some extent. A sorption test with groundwater confirmed that adsorbents can reduce vanadium to a very low concentration.

Keywords: Water treatment residual, Zerovalent iron, Kaolin clay, Adsorption, Groundwater

1. Introduction

Vanadium is one of the most industrially sought-after chemical elements because of its importance in the production of high-quality steel, which is the bedrock of modern technologies and development. As the quest for this toxic but important metal increases, the potential for pollution caused by vanadium is also imminent. The overall loading of vanadium in the environment is due mostly to natural sources, as vanadium is widely distributed in the Earth's crust while the main anthropogenic source of vanadium is fossil fuel [1]. The concentration level of vanadium is usually low in surface waters, but alarming levels have been reported, mostly in groundwater in different parts of the world, for example, 288 µg/l in El Hierro (Spain) [2], 2470 µg/l in the Pampean region (Argentina) [3] and 201 µg/l in Mt. Etna (Italy) [4]. Concerns over health effects from vanadium exposure have led national and regional governments to adopt more stringent limits concerning the permissible level for vanadium in drinking water. In Italy, the authority in charge of health regulations set the permissible limit of vanadium in drinking water to 140 µg/l in 2011 [2] while in the USA, the California Department of Public Health also set its notification limit for vanadium in drinking water to 50 µg/l [5].

Vanadium can exist in different oxidation states in the natural environment, but the most common is the oxidation state of +5 [1]. Pentavalent vanadium, V(V), has been recognized as the most toxic

species of all vanadium species. V(V) occurs as an anionic species when the pH value is higher than ~3. In regard to concentration, monovanadate species are said to be found in low-concentrated solutions, while polyvanadate species exist in higher concentrations [6]. Despite its complicated chemistry, vanadium is known to have a high affinity for many materials, such as activated carbon [7], organo-zeolites and iron-based adsorbents [8], which makes remediation through adsorption and ion exchange quite promising.

In recent years, attention has turned to the utilization of zerovalent iron (ZVI) as an adsorbent for metal removal. This can be attributed to its excellent adsorption characteristics and high capability in reducing recalcitrant contaminants [9]. Due to the recognized future potential of ZVI in the field of pollution remediation, there has been a continuous surge of innovative methods for synthesizing ZVI. However, the borohydride reduction technique is the most favoured, thanks to its procedural simplicity and homogeneity of product [10]. The small size of ZVI particles restricts its usage in environmental remediation and thus, to solve this problem, ZVI has been successfully immobilized on several support materials [9, 11]. For example, kaolin is an inexpensive support material and has proven to increase the stability of nanoparticles [12].

The primary aim of this study was to investigate the possibility of using iron extracted from groundwater plant sludge as a replacement for synthetic iron in ZVI modification. Due to the diminishing rate of available natural resources, utilization of so-called “waste resources” is environmentally and economically sustainable. Several studies have reported the use of water treatment residuals as adsorbents [13, 14, 15]. However, most papers dealing with this residue have mostly used it directly [16, 17] or after heat treatment and acid activation [18]. In this study, dissolving of the sludge was first optimized, since iron was needed in dissolved form. The extracted iron was used to produce a kaolin-supported ZVI (Slu-KZVI), which was tested as an adsorbent for vanadium removal in aqueous solution. The study compared the characteristics and vanadium adsorption performance of Slu-KZVI to those of a synthetic Fe-modified kaolin ZVI (Syn-KZVI) and to the best

of our knowledge, there is no publication on the use of kaolin-ZVI composite for vanadium removal. Other parameters investigated during this study included the effect of pH, contact time and initial vanadium concentration. The pre-adsorption and post-adsorption characterization of the adsorbents was performed by X-ray photoelectron spectroscopy (XPS), X-ray diffraction (XRD), Transmission electron microscopy (TEM) and N_2 adsorption/desorption measurements (surface area and pore size distribution). Since there is limited information on the behaviour of these adsorbents in real environments and when treating environmentally realistic concentrations, a preliminary test was also carried out with groundwater, to confirm whether the modified adsorbents could achieve a low vanadium residual concentration.

2. Materials and methods

2.1. Materials and reagents

Finnish kaolin clay was obtained from Puolanka, located in the Kainuu region of Finland. A <0.063 mm fraction (fine kaolin) was used in this study. Its chemical composition has been published earlier by Leiviskä et al. [19]. Iron-rich sludge was obtained from a groundwater treatment plant located in Oulu, in northern Finland. X-ray fluorescence (XRF) analysis of the sludge showed that its chemical composition was as follows: FeO (74.06%), SiO_2 (12.46%), MnO (5.06%), P_2O_5 (2.37%), CaO (1.18%), F (0.58%), Al_2O_3 (0.36%), K_2O (0.09%), S (0.07%), Na_2O (0.01%) and Ba (1910 ppm) as its major chemical content.

The chemicals and reagents used for the study were of analytical grade. Milli-Q ultrapure water was used throughout this study. $FeCl_3 \cdot 6H_2O$ (< 99%) and $NaBH_4$ (< 98%) were supplied by Fisher Scientific International Inc. (USA), whereas absolute ethanol (99.95%) was supplied by VWR International Oy (Helsinki, Finland). Synthetic vanadium solution was prepared from $NaVO_3$, manufactured by Sigma-Aldrich Chemical Corporation (USA). HNO_3 and HCl were supplied by Merck KGaA (Germany) and NaOH was supplied by VWR Chemicals.

A sample of groundwater (pH = 7.3) was taken from a Finnish groundwater treatment plant and spiked with vanadium (pH 6.2). The water quality characteristics of the spiked groundwater are presented in Table 3.

2.2. Synthetic KZVI (Syn-KZVI)

The preparation of Syn-KZVI was achieved through the Fe (III) reduction method as described by Rybka et al. [20]. Table 1 shows the exact mix proportion of the chemicals, reagents and materials used during the synthesis. Firstly, 150 ml of Fe solution was prepared by the dissolution of a weighed amount of $FeCl_3{\cdot}6H_2O$ in absolute ethanol. A consistent dissolution of the different percentages of Fe required in the adsorbents (10% and 25%) was achieved by ensuring that the weighed $FeCl_3.6H_2O$ contained an iron mass ratio equivalent to the weight percentage of Fe desired in the adsorbent. Secondly, 50 ml of 1 M $NaBH_4$ solution was prepared by dissolving a weighed amount of $NaBH_4$ in water. Then a measured amount of kaolin was added into a three-neck round-bottom flask into which the prepared 150 ml of Fe solution was added. The suspension was mixed for 10 min using a magnetic stirrer under an argon atmosphere. This was followed subsequently by the dropwise addition of the earlier prepared $NaBH_4$ solution. The obtained suspension was mixed for another 10 min. The $NaBH_4$ was added with an excess of 10% to ensure that Fe^{3+} was completely reduced to Fe^0. The chemical pathway for this reduction reaction is described in Eq. (1) below [20].

$$2FeCl_3 + 6NaBH_4 + 18\,H_2O \rightarrow 2Fe^0 + 6NaCl + 6B(OH)_3 + 21H_2 \qquad (1)$$

Black solids were formed concomitantly during the dropwise addition of $NaBH_4$. The produced black solids were later harvested by centrifuging the suspension for 10 min at 2500 rpm and then carefully decanting the supernatant. Finally, the recovered solids were washed three times with 20 ml of absolute ethanol and oven dried at 60°C for 8 h.

Table 1. Details of the reagents and materials used in the synthesis.

Adsorbent	**Ethanol (ml)**	**$FeCl_3 \cdot 6H_20$ (g)**	**Kaolin (g)**	**Fe (g)**	**$NaBH_4$ (g)**	H_2O (ml)	**Yield (g)**
10% Syn-KZVI	150	2.42	4.5	0.5	1.2	50	5
25% Syn-KZVI	150	6.04	3.75	1.248	2.78	50	5
	Ethanol (ml)	Slu-Fe (ml)	Kaolin (g)	Fe (g)	$NaBH_4$ (g)	H_2O (ml)	Yield (g)
10% Slu-KZVI	125	25	4.5	0.5	1.2	50	5
25% Slu-KZVI	88	62	3.75	1.248	2.78	50	5

2.3. KZVI from sludge (Slu-KZVI)

The procedure and parameters used for Slu-KZVI preparation were similar to those of Syn-KZVI except that the Fe was first extracted from the dried sludge (Table 1, Fig. S1). Before the reagent and procedure was chosen, five dissolution options were considered, entailing the dissolution of a weighed amount of sludge sample in 150 ml of ethanol (at 23 °C), in 1 M HCl (at 23 and 70 °C) and 1 M HCl + 1 M HNO_3 (at 23 and 70 °C) with 60 min mixing time. The Fe extracted from each of the dissolution trials was at a similar level, with the exception of the ethanol trial. The iron concentration in the ethanol solution was only about 0.02 mg/l (with 2 g sludge) whereas it was about 20-23 g/l in all the acid solutions (with 15 g sludge). The extraction method with 1 M HCl at room temperature was chosen because of its procedural simplicity and lower chemical and energy requirement.

To ensure that a mass equivalent of the Fe present in Syn-KZVI was dissolved from the sludge, XRF analysis was performed on the sludge to ascertain its FeO content and the amount of dissolvable Fe per gram of sludge was subsequently estimated. Atomic absorption spectroscopy (AAS) was used to confirm the dissolution of the desired Fe concentration (Perkin Elmer Aanalyst 400; standard methods SFS 3044 and SFS 3047). Then a weighed amount of sludge that could produce a Fe concentration ten times higher than that present in Syn-KZVI was added to 150 ml of 1 M HCl. After the desired high concentration was obtained, it was then diluted with absolute ethanol to achieve the targeted

lower concentration. The initial extraction of a higher concentration of Fe was a remedial effort to minimize the effect of HCl on the synthesized adsorbent since its presence might have impeded reduction. The subsequent procedure and parameters were the same as those described for Syn-KZVI, apart from the fact that the required drying time was noticed to be shorter with Slu-KZVI (6 h) when compared with the time required to dry the Syn-KZVI (8 h). Considering that the HCl needed for Fe dissolution is widely available and cheap, and it was possible to optimize the Fe concentration easily. This extraction procedure was observed to present not only a viable method of extraction but also a cheaper alternative to industrially produced iron. Nevertheless, it is noteworthy that the extracted Fe needs to be freshly prepared before KZVI modification for optimal performance.

2.4. Characterization and water analysis methods

Prior to XRD analysis, samples were ground to very fine particles to obtain a uniform particle size. Probing of the crystalline morphology of the adsorbent was performed with a RIGAKU Mini-flex 600 X-ray powder diffractometer with a Cu-kα (λ=1.5418Å) radiation configuration. The patterns generated from the diffraction were recorded within the range of 2−75 °2θ with an increment count of 0.05 °2θ. A Bruker AXS S4 Pioneer X-ray XRF spectrometer was employed to ascertain the chemical composition of the groundwater sludge. XRF analysis was performed by pelletizing the sludge. The pellets were produced with the use of boric acid as a binder.

XPS characterization was performed with a Thermo Fisher Scientific ESCALAB 250xi with an X-ray source from a rotating monochromatic Al anode, generating an X-ray beam at 1486.6 eV. Binding energy (BE) was corrected by charge shifting, with the assumption that the binding energy for adventitious carbon is 284.8 eV. All spectra were fitted using a Shirley-type background.

Transmission electron microscopy (TEM) and energy dispersed spectroscopy (EDS) analysis were carried out using a JEOL 2200 FS with selected area electron diffraction, operated at an acceleration

voltage of 200 KV. Samples were dispersed in 99.9% laboratory grade ethanol before deposition on Cu grids coated with lacey carbon.

The BET (Brunauer, Emmett and Teller) surface area and pore size distributions were calculated from N_2 isotherms measured with an ASAP 2020 surface area and porosity analyser (Micromeritics). The surface area was measured by the nitrogen adsorption technique at -195.86°C in a 0.01–0.1 relative pressure range. Before analysis, the samples were out-gassed in a vacuum for 12 h at a temperature of 100 °C. The pore size distribution was calculated by analysing the desorption branches of the isotherm using the BJH (Barrett-Joyner-Halenda) method.

The pH measurement was made using a VWR Phenomenal pH 1000 L. In batch experiments with the synthetic vanadium solutions, the vanadium concentration was analysed using graphite furnace atomic absorption spectroscopy (GFAAS Perkin Elmer Analyst 600) with argon, following standard method SFS 5074: 1990. In groundwater treatment tests, Cl, F and SO_4^{2-} were analysed using ion chromatography (SFS-EN ISO 10304-1:2009); NO_2-N, NO_3-N, NH_4-N and PO_4-P were analysed using a continuous flow analyser (SFS-EN ISO 13395:1997, SFS-EN ISO 11732:2005, SFS-EN ISO 15681-2:2005); and the concentration of elements in the groundwater was analysed using inductively coupled plasma mass spectrometry (ICP-OES) (SFS-EN ISO 17294-2:2005). An Fe and Mn leaching test was also conducted using ICP-OES (SFS-EN ISO 11885:2009).

2.5. Batch adsorption tests

The efficiency of the adsorbents was tested by means of batch sorption tests using synthetic vanadium solutions. All experiments were performed at room temperature and run in duplicates. The effect of different products was studied with 20 mg/l vanadium solution without pH adjustment (initial pH ~5) and using a dosage of 2 g/l. After a shaking period of 24 h, the solid and solution phases were

separated by centrifugation at 2500 rpm for 10 min. The analytical samples were taken from the supernatant solution, acidified with 50 µl of 37% HCl and stored at 6 °C.

The maximum capacity of the adsorbents was studied using varying vanadium concentrations (10-140 mg/l; pH ~5), a dosage of 2 g/l and 24 h contact time. The effect of pH on vanadium removal was studied using a dosage of 2 g/l, 24 h contact time and initial vanadium concentration of 20 mg/l. The pH of the samples was adjusted to the desired pH value with 0.5 M HCl and 0.5 M NaOH. The effect of contact time was studied using a dosage of 2 g/l and initial vanadium concentration of 20 mg/l without pH adjustment (pH~5). Tests with spiked groundwater were carried out using a dosage of 1 g/l, 2 h contact time and without pH adjustment. An Fe and Mn leaching test was performed for the samples obtained from the pH test.

3. Results and discussion

3.1. Studies on synthesis constituents and KZVIs of different wt%

According to the adsorption results presented in Fig. 1, kaolin clay was found to have exhibited the poorest removal rate; this is caused mainly by its lack of anion exchange capacity [20, 21]. The amount of V adsorbed by iron sludge was quite significant when compared to kaolin, as the result revealed that more than 65% of the studied vanadium content (20 mg/l) had been removed. This performance could be attributed to the high percentage of iron present in the sludge (74.06% FeO). Iron compounds provide surface sites on which anions form outer-sphere complexes. Previous studies have also reported good performance of water treatment sludges as adsorbents. For example, Gibbons et al. [11] reported an impressive phosphate removal when using different water treatment residues. Despite its high removal capacity, it might not be possible to use raw sludge directly as an adsorbent in sensitive applications, because it very often contains some unknown inorganic impurities, which might lead to cross-contamination. Another advantage of modified Slu-KZVI over raw sludge is that

numerous publications have reported the ability of ZVI to simultaneously remediate quite a number of pollutants that might coexist with the targeted contaminant.

Fig. 1 also shows that an increase in ZVI loading on kaolin from 10% to 25% resulted in improved vanadium removal efficiency for Slu-KZVI from 66.5% to 72.5%, whereas Syn-KZVI exhibited increased removal from 79.6% to 92.0%. This improved performance could be best attributed to an increase in the surface area of the composite. Although the adsorption results had revealed that an increment of zerovalent iron in the modified adsorbents might have led to better performance regarding vanadium removal, further experimental tests were performed only on the 10% modifications because of their close adsorption efficiency when compared with 25% KZVI. It was also considered that less chemicals and materials would thus be needed for synthesis and to achieve a relatively reasonable level of performance.

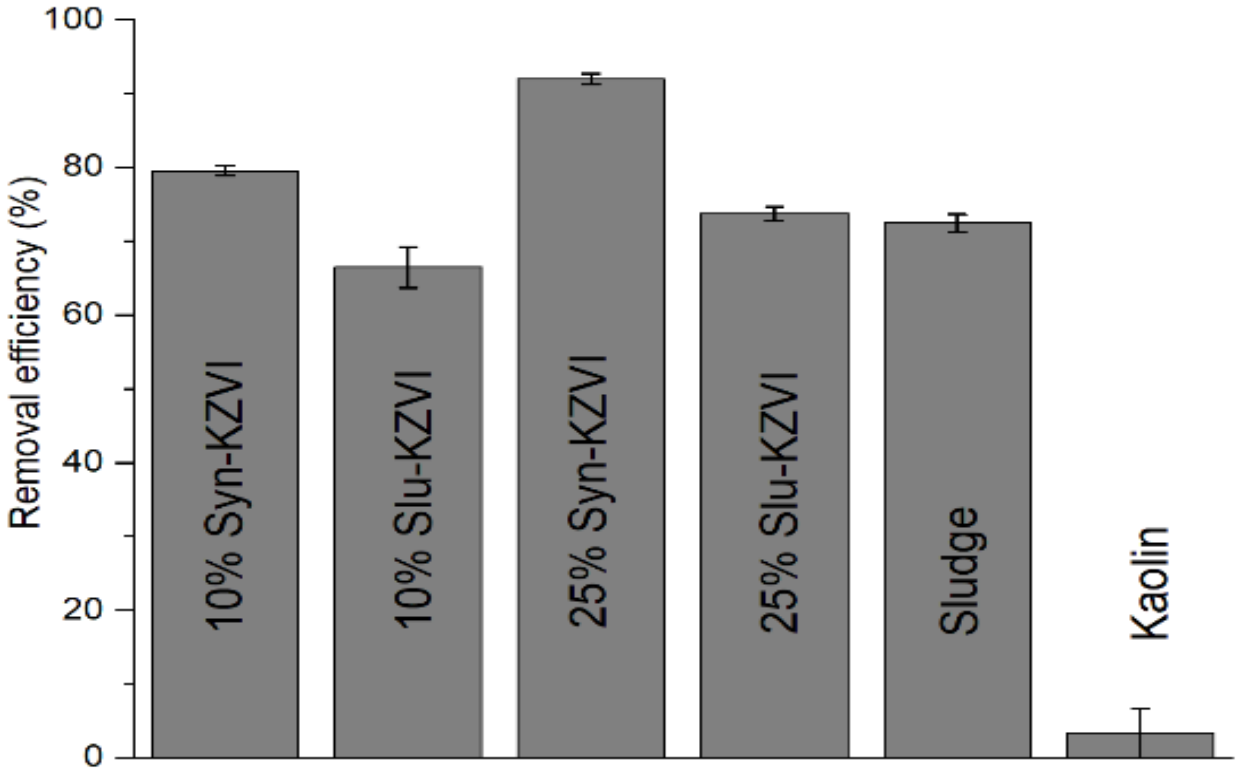

Fig. 1. Removal efficiency of vanadium versus adsorbent and ZVI content (Adsorbent dose: 2 g/l; Solution pH: initial pH ~5 and final pH ~8; Solution V concentration: 20 mg/l; Contact time: 24 h; Temperature: 21±3 ^{o}C).

3.2. Characterization of kaolin and modified adsorbents

The kaolin clay sample support used in the study showed a 7.2 Å basal (d_{001}) reflection in the XRD pattern typical for kaolin group minerals. Peaks of quartz (4.25 Å and 3.34 Å) and illite (9.96 Å and 4.97 Å) were also observed. The diffraction pattern displayed in Fig. 2 indicates the successful dispersion of zerovalent iron on the surface of kaolin. An increase in the intensity of the basal spacing could be observed in both 10% and 25% KZVIs at 2.03 Å. However, the increment was noticed to be more prominent in 25% KZVI than in 10%, and these trends were quite similar to those earlier reported by Üzüm et al. [22] and Rybka et al. [20]. Rybka et al. [20] also reported the presence of zerovalent iron at basal spacing of 2.92 Å and 2.03 Å, which was observed to be featureless in the 10% modified adsorbents but quite prominent in the 25% adsorbents. The lack of shift of the 7.2 Å basal spacing of the modified adsorbents indicated that ZVI particles were synthesized exclusively on the kaolin and intercalation did not occur.

Physical observation of the XRD pattern for the 25% KZVI adsorbents showed the emergence of irregular peaks (3.91 Å, 2.79 Å and 1.49 Å) when compared with the base material (kaolinite) and 10% ZVI modifications. However, the reasons for the emergence of these new peaks in the 25% KZVI adsorbents were not investigated in this study.

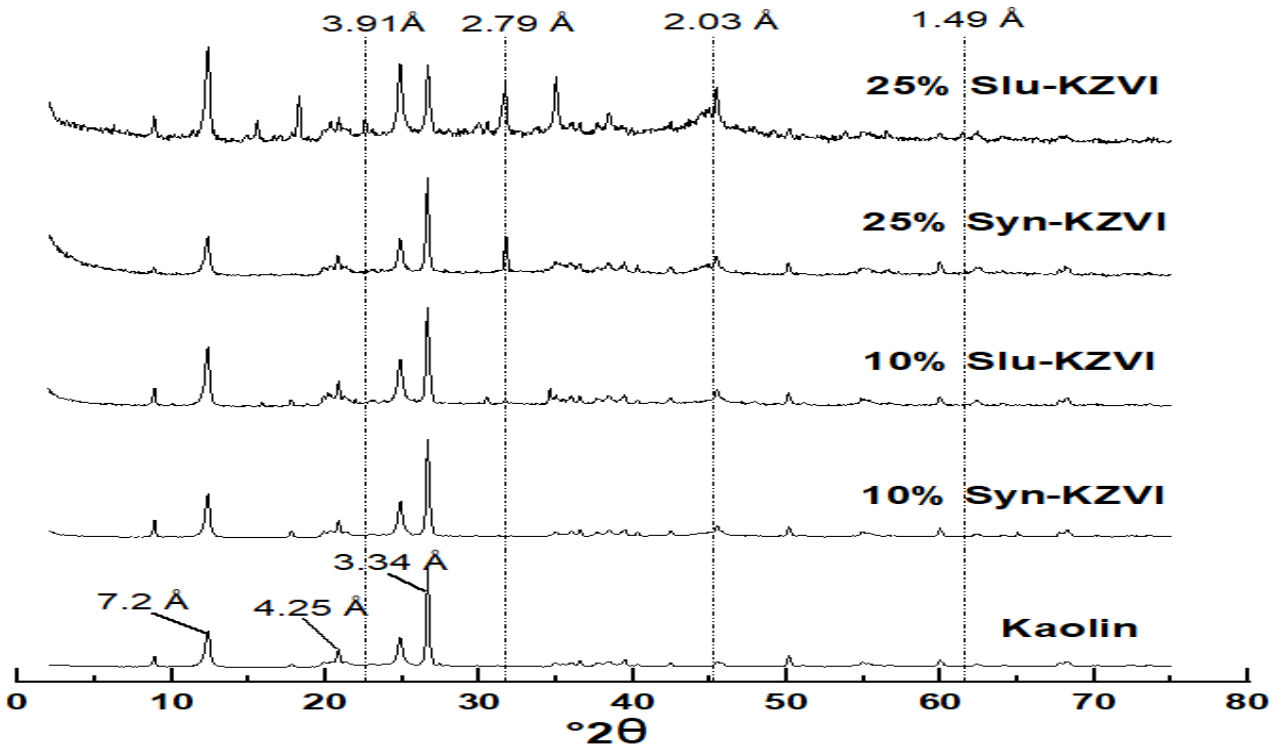

Fig. 2. XRD patterns of kaolin, 10% KZVIs and 25% KZVIs.

The elemental peaks identified in the XPS wide spectra confirmed the presence of Al, Si, Mg, Fe, Cl, B, Na and C in both adsorbents (Fig. S2). Al and Si derived mainly from kaolin clay while Fe, Cl, B and Na originated from the use of Fe and $NaBH_4$ to synthesize ZVI. The sodium borohydride employed for the reduction of Fe during the ZVI synthesis phase is known to be highly soluble, so it was expected to have been removed during the washing stage. Nonetheless, some boron was still present in the modified adsorbents, although it could be removed by more efficient washing (see discussion of boron leaching in Section 3.7). The carbon present in the spectra could have emerged due to exposure to carbon dioxide and hydrocarbons during sample preparation. The XPS analysis for Slu-KZVI indicated the presence of additional elements such as P and Ca, which were not present in the Syn-KZVI adsorbent. The presence of these elements was expected as XRF analysis had revealed that P and Ca were present in the sludge in significant amounts.

The surface elemental content obtained from the XPS analysis gives more clarification on the reason why Syn-KZVI had been able to out-perform Slu-KZVI. It might have been due to the higher iron

content (12.9% with 10% Syn-KZVI and 11.6% with 10% Slu-KZVI; as wt%). The percentile of Fe 2p should comprise oxidized and un-oxidized Fe (ZVI). Iron oxides provide surface sites on which metals forms outer-sphere complexes, whereas ZVI can sequester contaminants through oxidation (in the presence of dissolved oxygen), reduction, precipitation and adsorption [23]. However, the accuracy of the values for proportioning the ratio of chemical elements in Slu-KZVI was questionable due to the overlapping peaks of different chemical elements. For example, the B1s peak at ~193 eV was found to overlap with that of P 2s; therefore, the exact value of boron could not be obtained, and thus other percentage values might also have been incorrect.

A detailed Fe 2p XPS spectrum comparison for both classes of adsorbent modification is displayed in Fig. 3. For Syn-KZVI, binding peaks at 711.9 eV ($2p_{3/2}$) correspond to the peak of oxidized iron [24], while the small peak at ~708 eV indicates the existence of ZVI [25]. A similar Fe 2p structure can also be seen for Slu-KZVI in Fig. 3. However, a shift in the peak position of $2p_{3/2}$ from 711.9 eV to 712.5 eV was noticed. In addition, the ZVI peak is prominent in the Fe 2p spectrum of Syn-KZVI but less intense with Slu-KZVI. This is believed to have been caused by the presence of a lesser amount of ZVI on the surface of Slu-KZVI than on the surface of Syn-KZVI. Nonetheless, the proportion of oxidized iron on the surface is high with both adsorbents and this is in line with previous results by Yayayürük and Yayayürük [26].

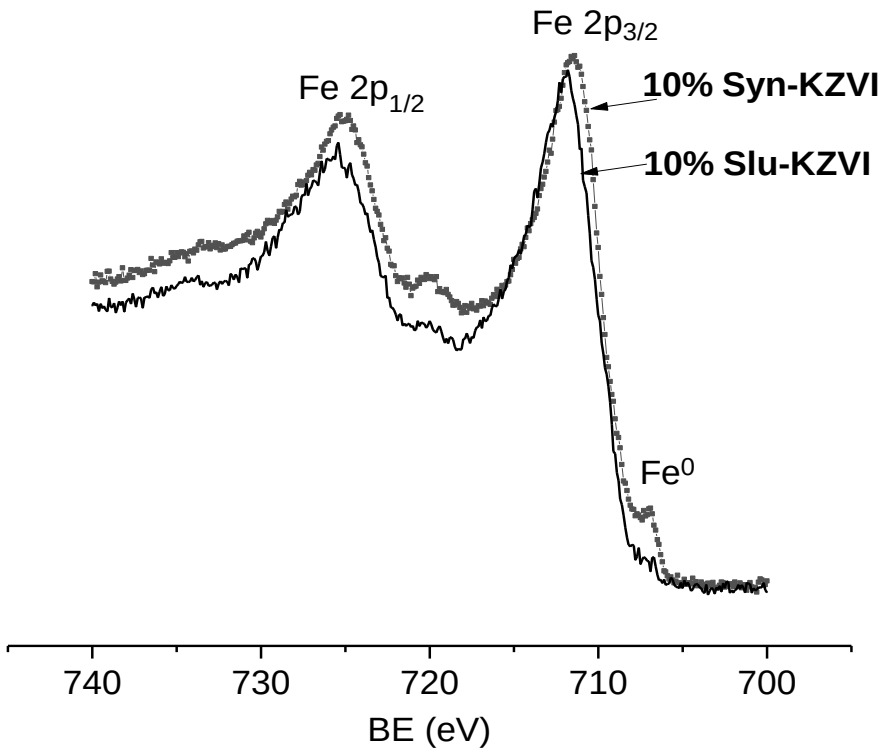

Fig. 3. Comparison of 10% Slu-KZVI and 10% Syn-KZVI Fe 2p XPS spectra.

Transmission electron microscopy (TEM) was used to probe the morphology of the synthesized samples. The TEM image displayed in Fig. 4(a) for kaolin indicates that it is mostly composed of anhedral particles, whereas EDS analysis of the image revealed an alumina-silicate composition consistent with phases identified by XRD. The kaolin group minerals present in the sample showed diverse morphology, mainly including platy particles, although minor amounts of halloysite-like tubes could also be observed. The TEM images in Fig. 4 (b-c) corresponding to Syn-KZVI and Slu-KZVI, respectively, display a clustered series of quasi-spherical structures with a distinct contrasting core-shell morphology, which is consistent with earlier findings [27, 28]. The chain-like morphological structure depicted in the figures has been attributed mainly to a magnetic dipole-dipole interaction among the ZVI nanoparticles [28].

The EDS was used on a high-resolution image to obtain the quantitative chemical composition of the core and shell of some individual nano-chain particles, which revealed that oxygen, iron, and boron were the most prominent elements in the shell, while the core consisted mainly of iron. This corroborates the widely reported formation of oxidized iron on the surface of ZVI. The satellite images in Fig. 4 (b-c) also revealed the thickness of the oxidized shell for both classes of modified adsorbents. It is essential to take into account that the depth of this amorphous layer is minimal when considering the reactivity of synthesized nanoparticle. Furthermore, the presence of boron indicates the ineffectiveness of the ethanol washing procedure. Interestingly, the Slu-KZVI image portrayed in Fig. 4(c) also reveals that no visual change occurred to the morphology of the kaolin in that its pristine anhedral structure was unaltered by ZVI synthesis, as it is visible in the background with an overlaying cluster of iron nanoparticles.

A

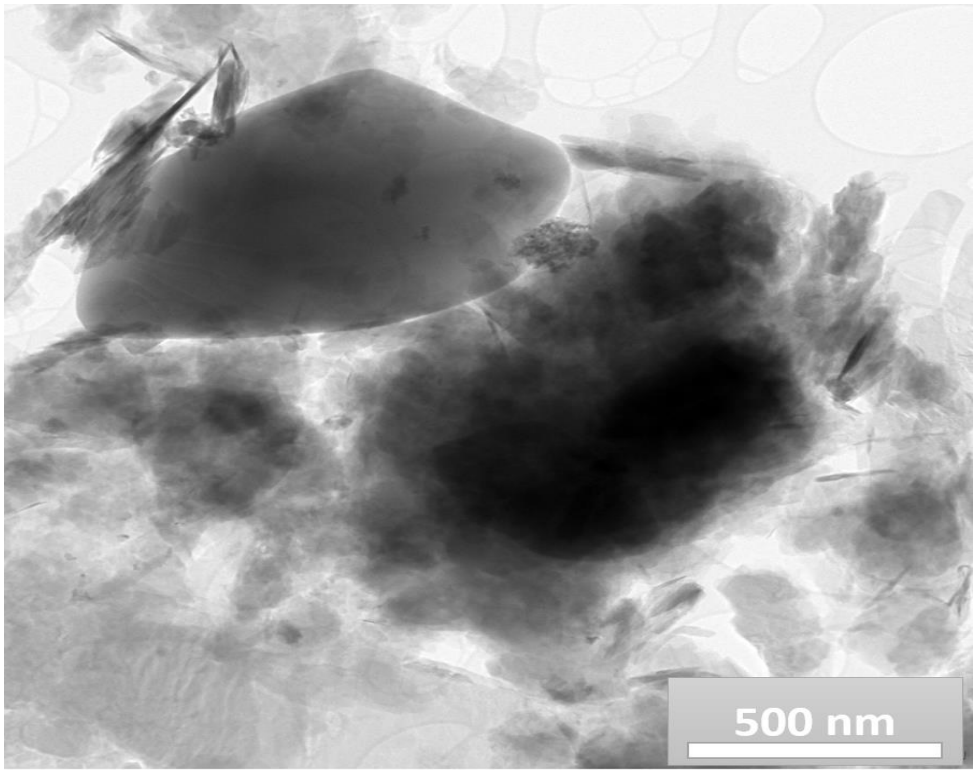

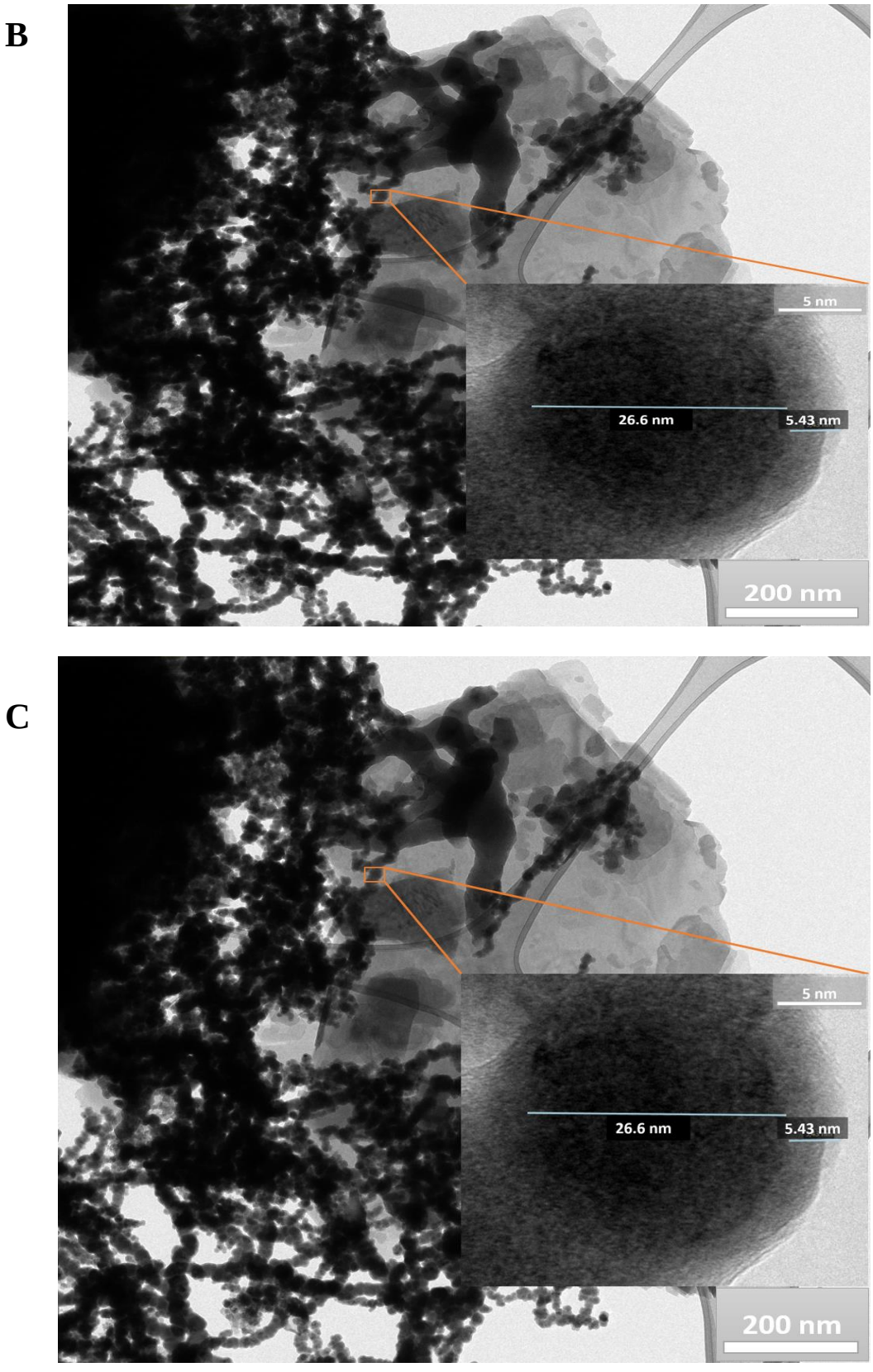

Fig. 4. TEM images of a) kaolin, b) 10% Syn-KZVI, c) 10% Slu-KZVI.

The specific surface area, pore volume and pore diameter of the modified adsorbents are presented in Table 2. The results revealed a positive correlation between the surface area and wt.% of Fe. These values show a modest surface area with the exception of 25% Syn-KZVI in comparison with bare ZVI or many other ZVI composite applications [9]. The low surface area is believed to have been induced after conjugation with kaolin, which is known to have a very low specific surface area [29]. The pore size distribution graph presented in the supplementary material (Fig. S3) shows that the pore size of the adsorbents ranged from 1 to 140 nm and that most were within the mesopore range (2-50 nm). It also revealed that the 10% Fe adsorbents had a broader size distribution than their 25% counterpart, but that 25% KZVI possessed greater pore volumes.

Table 2. Surface area, pore volume and pore diameter of adsorbents.

Adsorbent	BET Surface area (m^2/g)	BJH pore volume (cm^3/g)	BJH desorption average pore diameter (nm)
10% Syn-KZVI	9.2	0.0452	17.7
25% Syn-KZVI	52.0	0.1650	8.9
10% Slu-KZVI	14.3	0.0679	18.0
25% Slu-KZVI	18.1	0.0696	15.8

3.3. Effect of initial concentration

Fig. 5 shows the performance of the adsorbents (10% Fe) when the initial concentration of the vanadium increased from 10 to 140 mg/l while the other parameters were kept constant. Both adsorbents were able to achieve a uniform 4 mg/g (>82%) removal rate from a 10 mg/l vanadium solution (dosage 2 g/l). During a further adsorbate increment, both classes of KZVI modifications showed an upward trend in their vanadium uptake and a maximum capacity of ~15 mg/g was reached. The capacity obtained is clearly much lower than that earlier reported for bare nanosized ZVI (q_{exp} = 324 mg V /g) [26] since kaolin is assumed not to adsorb vanadium. On the other hand, the capacity can be adjusted by the amount of ZVI loading on the support material. In general, the adsorption capacities of ZVI-based materials (both bare and composites) have been found to vary widely, ranging from a few milligrams to several hundred milligrams per gram of material [9].

The adsorption data was fitted into different adsorption isotherm models, namely the Langmuir, Freundlich, Sips, Dubinin–Radushkevich and Redlich-Peterson models (Table S1). The Langmuir model fitted best with the adsorption data for the 10% Slu-KZVI, suggesting a monolayer adsorption during the adsorption process (Fig. S4). For the 10% Syn-KZVI, the Freundlich model showed the best fit, which indicates sorption on a heterogeneous surface (Fig. S5).

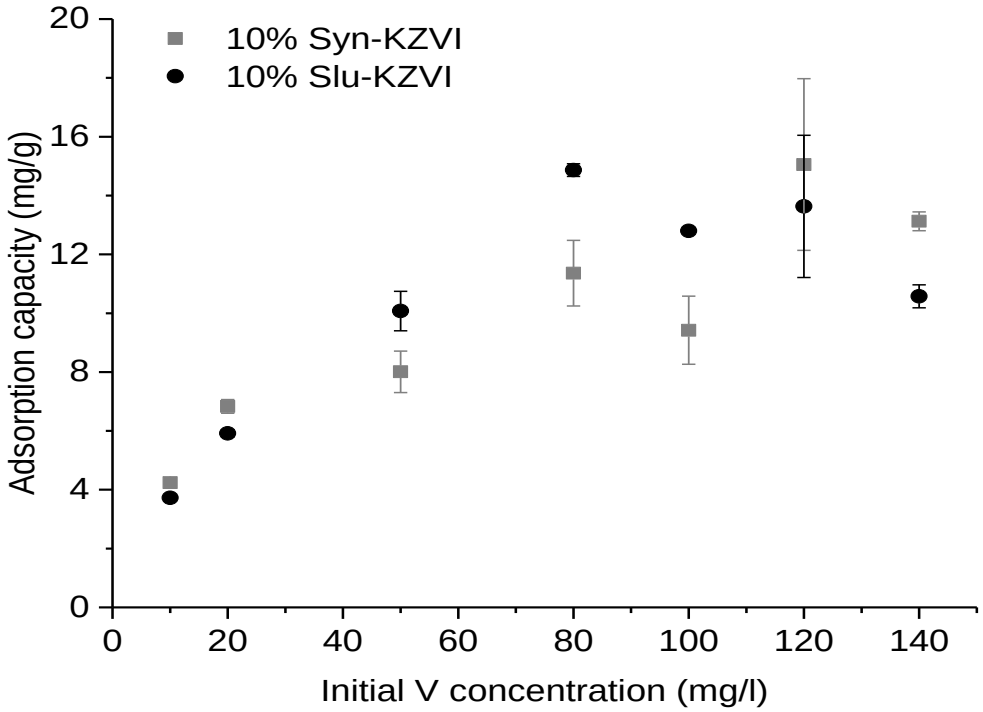

Fig. 5. Effect of initial vanadium concentration on the adsorption capacity (Adsorbent dose: 2 g/l; Solution pH: initial ~pH 5 and final ~pH 8; Contact time 24 h; Temperature; 21±3 °C).

3.4. Effect of pH

The pH may play a crucial role in the uptake of adsorbate by an adsorbent from an aqueous solution. More importantly for this study, vanadium is known to exist as a cationic species at very low pH values and as an anionic species at pH values above ~3 [6]. In addition, at pH values lower than the isoelectric point (IEP) of the adsorbent, vanadium adsorption is favoured due to a positive net charge. ZVI has an IEP at pH 7.7 [30]. The results from the experiments showed a strong correlation between pH and the removal capacity of the modified adsorbents (Fig. 6). Both classes of the modified

adsorbent were recorded to have achieved above 98% removal during the test with a pH 3 solution, whereas in cases with pH values of 5, 7, 9 and 10, both adsorbents showed a removal efficiency of over 60% from the 20 mg/l vanadium solution. This trend was in good agreement with previous studies [31, 32]. Kanel et al. [28] reported a 100% removal of As(V) by ZVI at pH 3 (dosage 0.1 g/l, initial As(V) concentration 1 mg/l), but its efficiency was reduced to around 85% at pH 9.

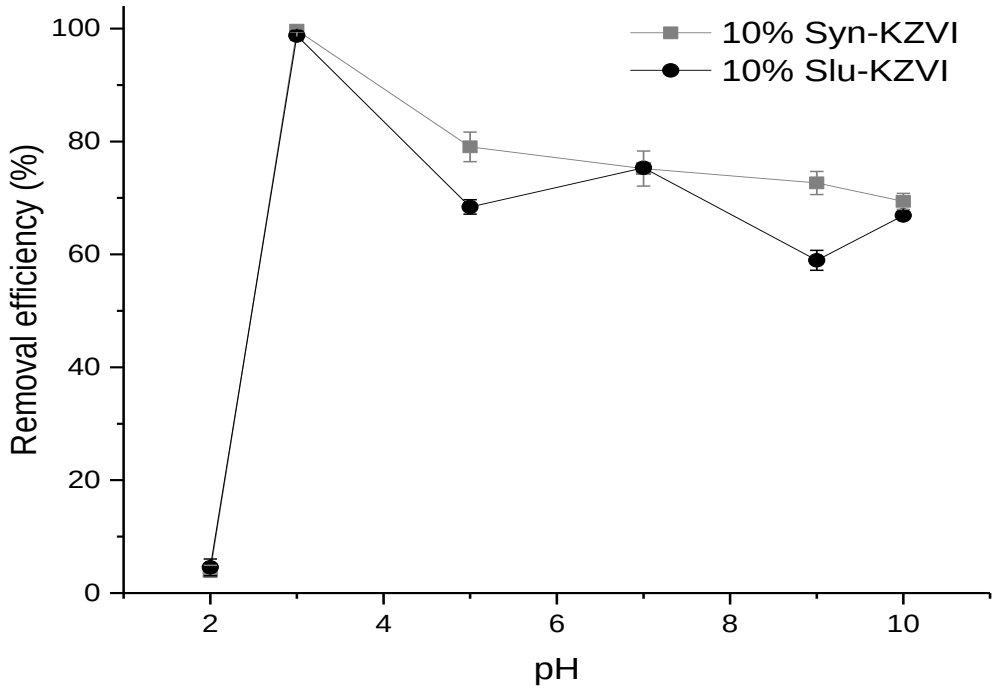

Fig. 6. Effect of pH on the vanadium removal rate by 10% Syn-KZVI and 10% Slu-KZVI (Adsorbent dose: 2 g/l; Solution concentration: 20 mg/l; Contact time: 24 h; Temperature; 21±3 ^{o}C).

A very low adsorption was recorded when the adsorbents were tested at pH 2. Adsorption results from this experiment revealed that the removal percentage for 10% Syn-KZVI and 10% Slu-KZVI was only 4.5% and 3.9%, respectively. Physical observation of KZVI samples during the test with this extremely acidic pH showed that the adsorbents were destroyed, as a distinctive separation of black particles of ZVI and kaolin was observed. However, this trend was expected, as an extreme pH value leads to the dissolution of Fe^0 and Fe oxides, resulting in an increase of Fe concentration in the solution [33].

3.5. Effect of contact time

Vanadium uptake by both classes of modified adsorbents occurred uniformly with time. The results from Fig. 7 indicate that the interaction between vanadium and the modified adsorbents was rapid, as maximum uptake was achieved within 30 min. On average, the vanadium uptake was observed to be somewhat higher with Syn-KZVI, which could be attributed to the availability of more binding sites, facilitating better interaction between adsorbate and adsorbent. Fast kinetics for vanadium uptake were also found with nanosized ZVI, which reached equilibrium in about 10 min [26]. According to Azzam et al. [34], the removal equilibrium of several metal cations by ZVI was achieved after 20-30 min.

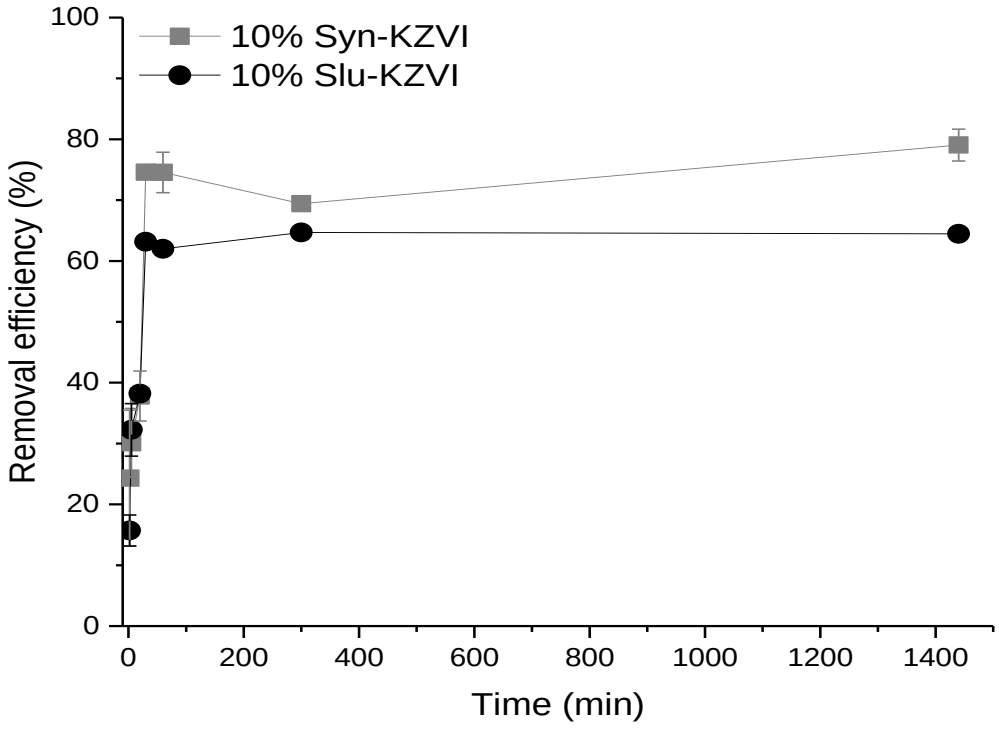

Fig. 7. Effect of contact time on vanadium adsorption (Adsorbent dose: 2 g/l; Solution pH: initial pH ~5 and final pH ~8; Solution concentration: 20 mg/l; Temperature: 21±3 °C).

3.6. Characterization of vanadium-treated adsorbents

XRD and XPS analyses carried out for both adsorbents after adsorption indicated similar structural changes. The XRD pattern (showing only Slu-KZVI samples, Fig. 8) indicates the oxidation of ZVI and formation of vanadium oxides. The presence of vanadium in the treated sample was confirmed by the newly emerged peaks at 2.51 Å and 1.43 Å, which presumably originated from the vanadium oxide phase [35].

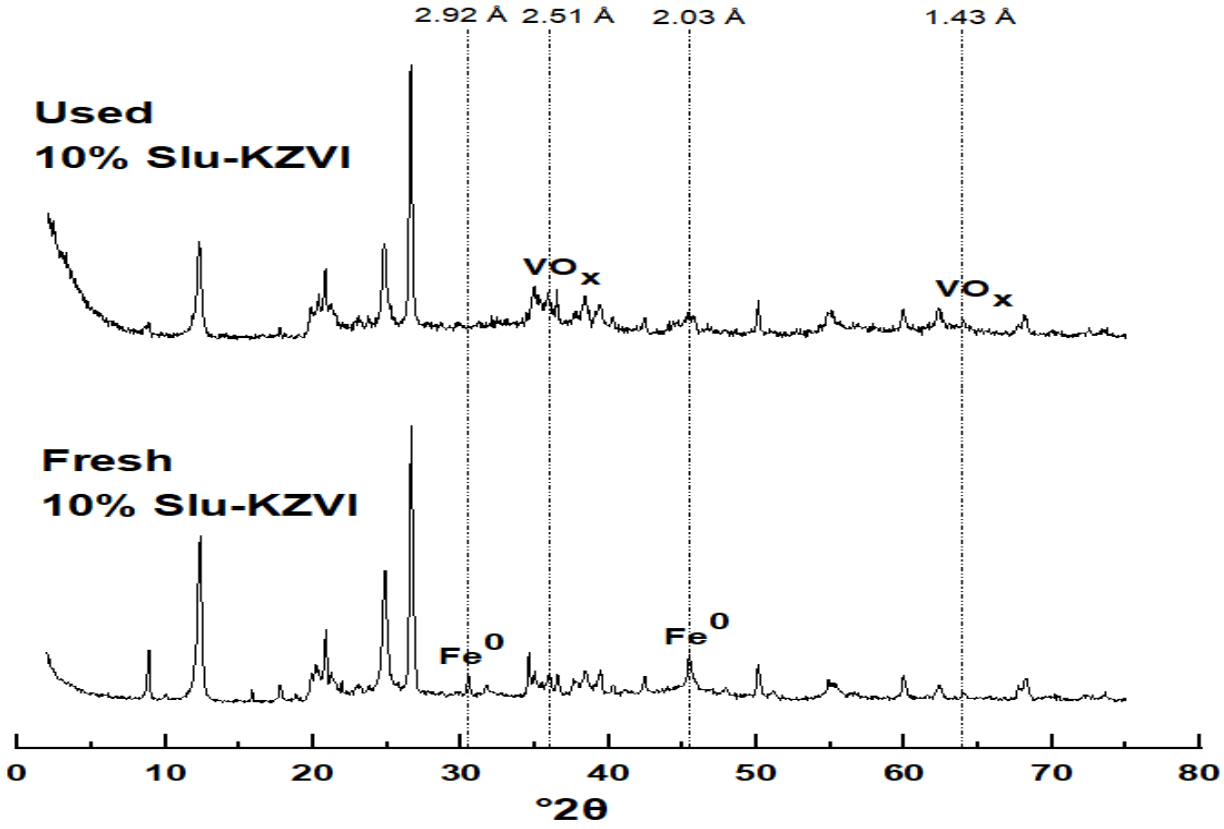

Fig. 8. XRD overlaying comparison of fresh and used 10% Slu-KZVI.

Prominent peaks at 2.92 Å and 2.03 Å assigned to the ZVI in the fresh sample were found to be imperceptible in its V-loaded counterpart. Furthermore, the small peak corresponding to ZVI in the Fe 2p spectra (Fig. 3) was missing in the spectra of vanadium-treated adsorbents. In addition, an increase was observed in the intensity of the shake-up satellite at ~720 eV between the Fe $2p_{3/2}$ and Fe $2p_{1/2}$ envelopes for the V-loaded samples; it was speculated that this was due to the precipitation of Fe oxides, most possibly hematite (α-Fe_2O_3) [36] (Fig. S6). These findings indicate that ZVI was oxidized on the surface of adsorbents, and the simultaneous V(V) reduction and Fe oxidation (redox)

reactions might be the mechanism for vanadium uptake. However, the V 2p spectrum of the adsorbents after exposure to a 20 mg/l vanadium solution showed V $2p_{3/2}$ at 517.4-517.5 eV (Fig. 9), which corresponds to the binding energy of oxidized vanadium V(V) [37]. This suggests that the vanadium uptake was not due to the reduction of vanadium, but rather to the binding of vanadium by surface hydroxyl groups. The V 2p binding energies were also in agreement with the results reported by Yayayürük and Yayayürük [26], who used the same procedure to synthesize ZVI and suggested surface complexation as the main mechanism for vanadium binding.

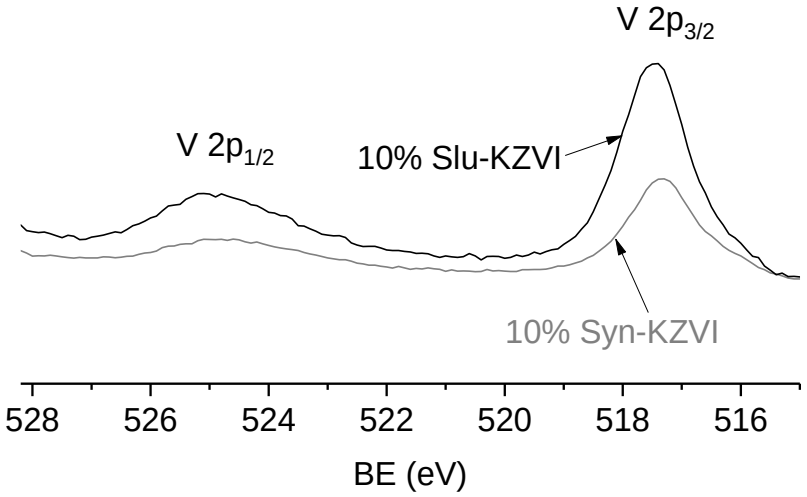

Fig. 9. V 2p XPS spectra obtained from V-loaded samples.

The TEM microphotographs of the vanadium-treated Syn-KZVI and Slu-KZVI are displayed in Fig. 10(a) and (b), respectively. It is possible to observe the disappearance of the Fe-rich core in Fig 10 (c) for the fresh sample and 10 (d) for the V-treated sample (Slu-KZVI is shown), which indicates the consumption of reactive metallic iron and an increase in oxygen due to iron oxide formation [28].The EDS maps of these samples, in Fig 10(e) and (f) for the synthetic and sludge KZVIs, depict a homogeneous distribution of vanadium over Fe-concentrated areas. A change in the crystallinity and asymmetry of the V-loaded samples was also observed. These patterns were consistent with the earlier literature [32] when ZVI was used as an adsorbent for aqueous As.

A

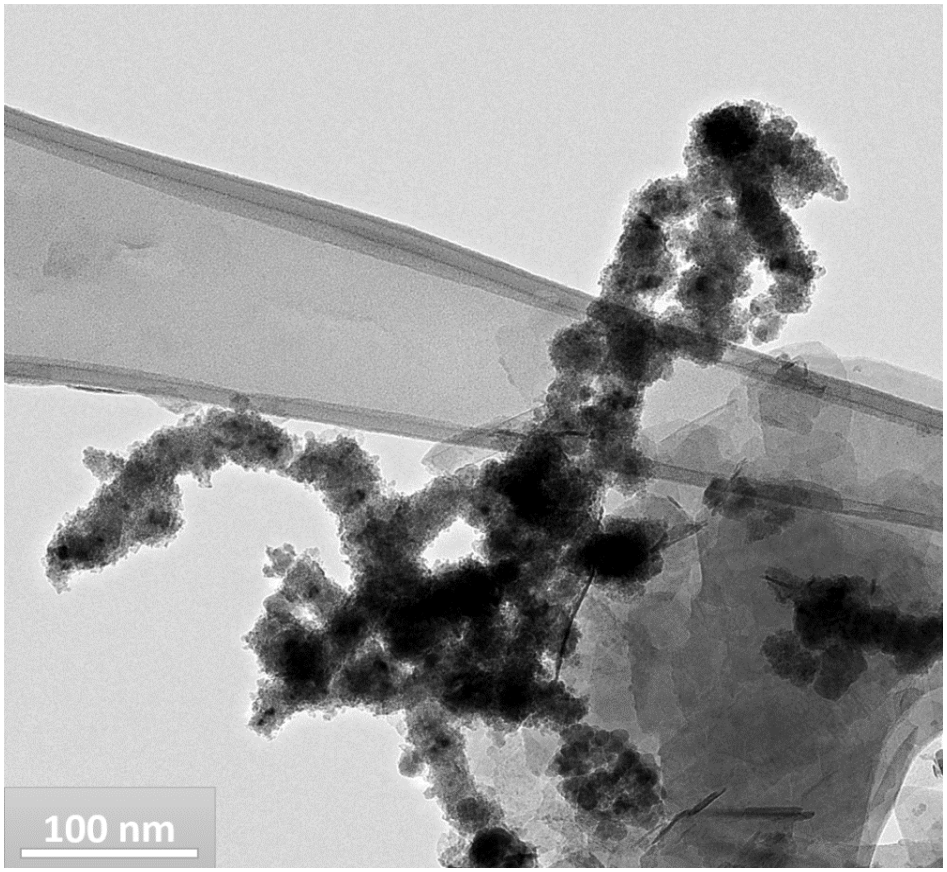

B

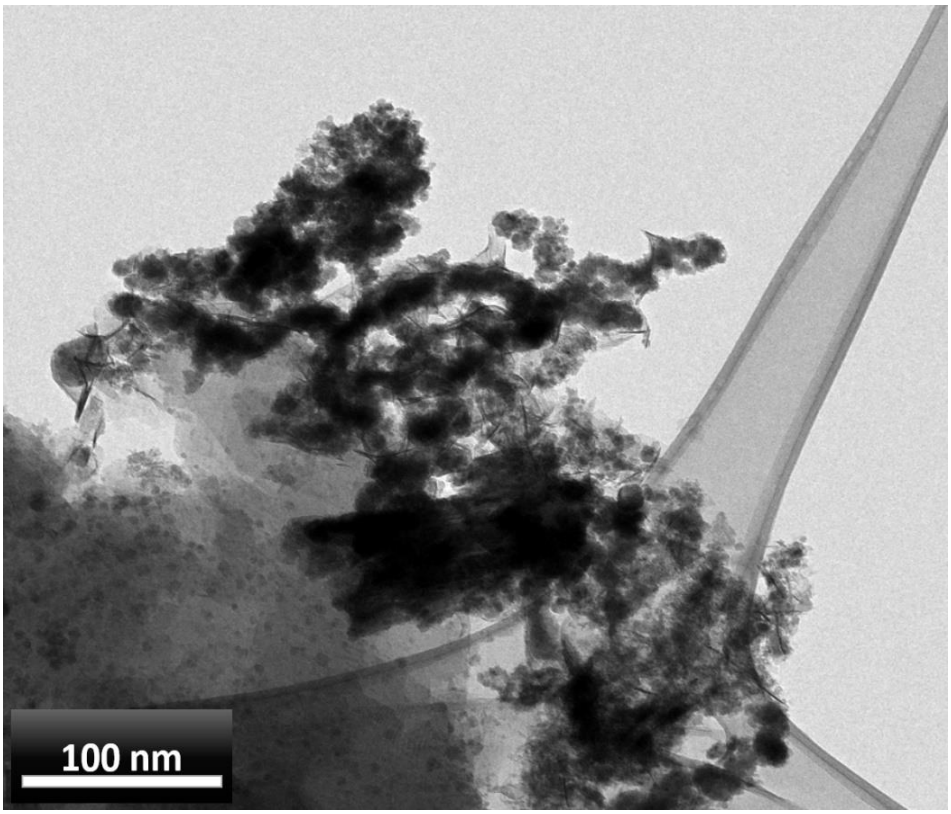

C

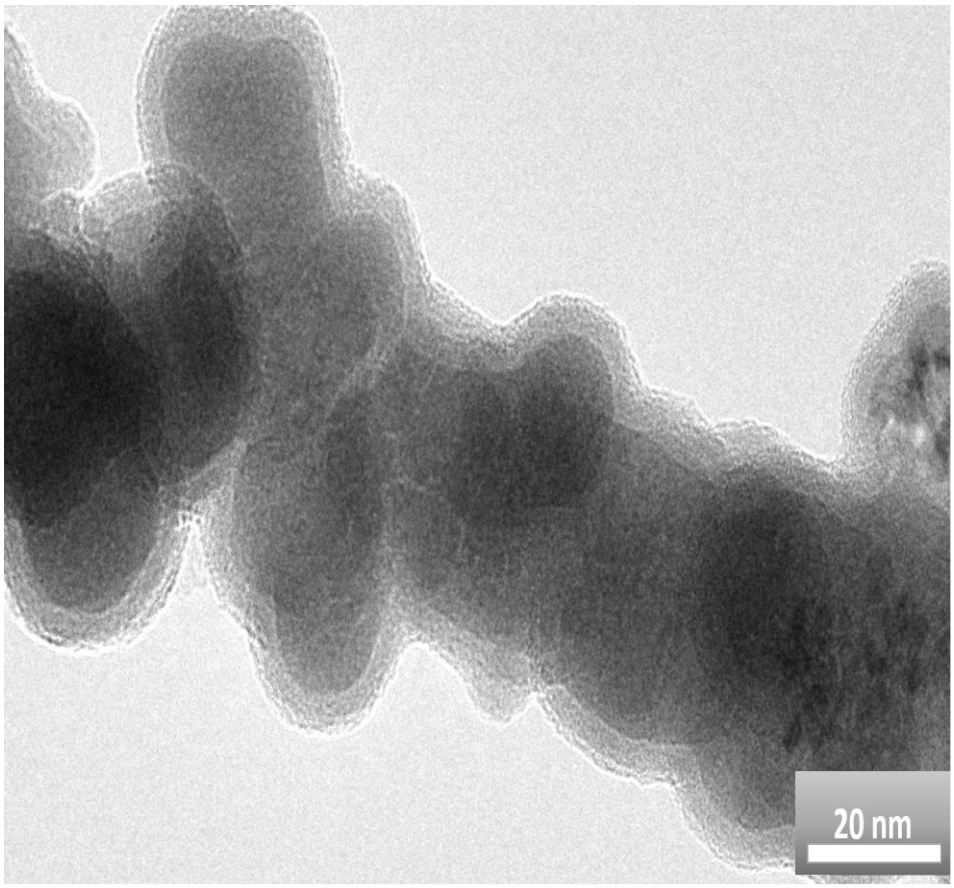

D

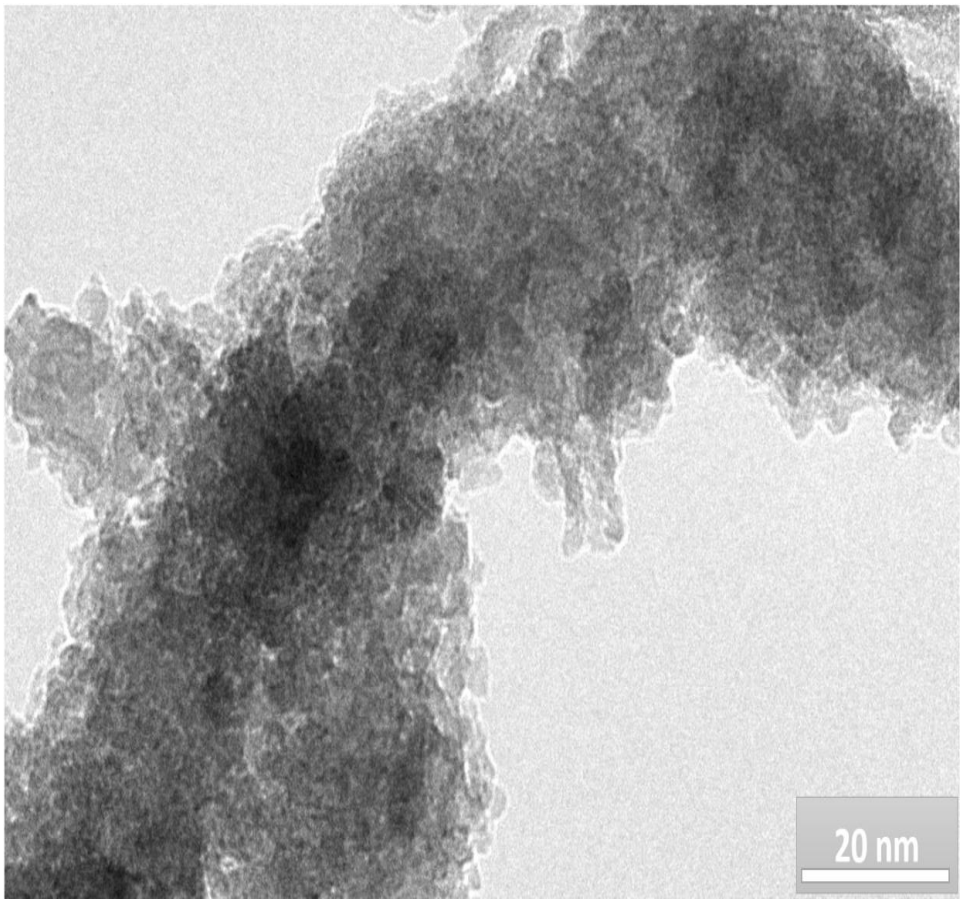

E

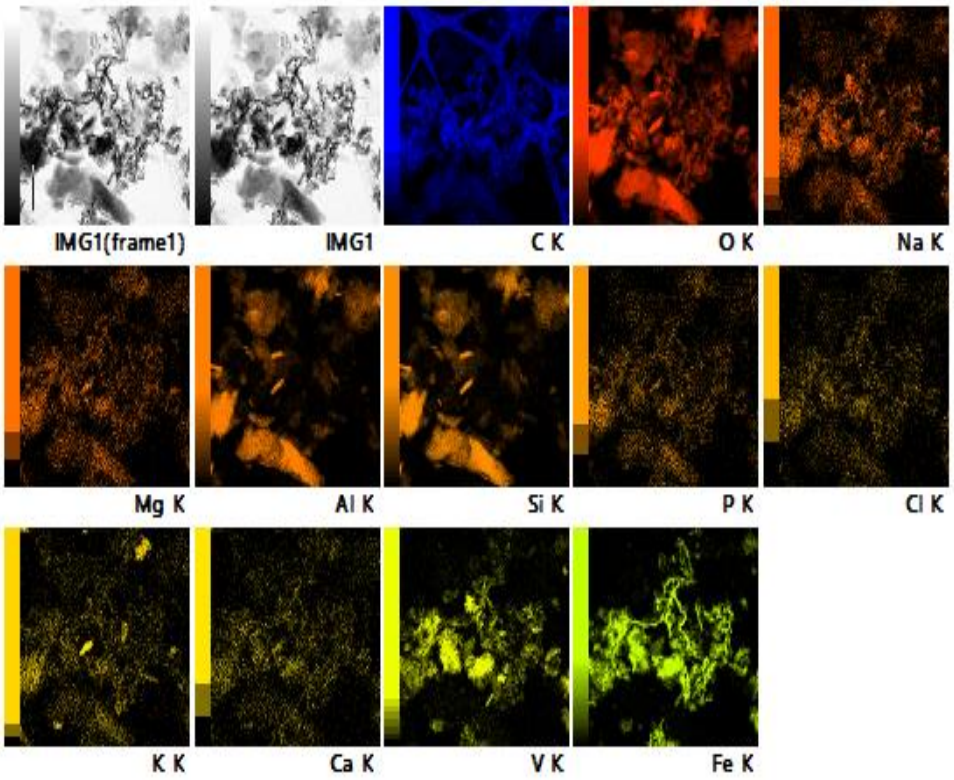

F

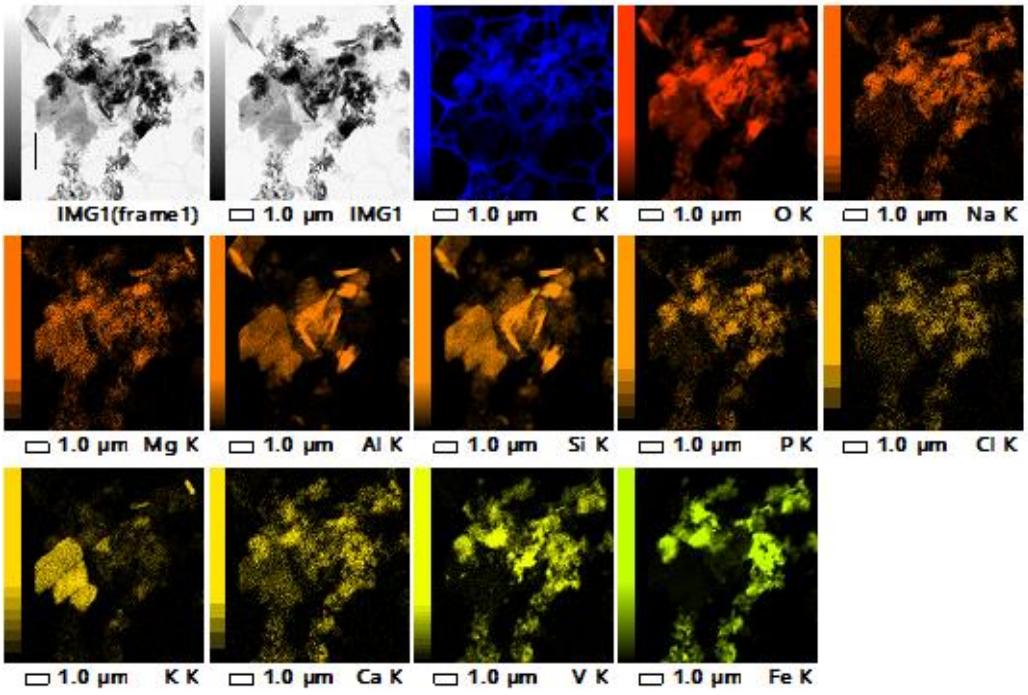

Fig. 10. TEM images of a) V-loaded 10% Syn-KZVI, b) V-loaded 10% Slu-KZVI. High resolution TEM images of c) Fresh 10% Slu-KZVI, d) V-loaded 10% Slu-KZVI and EDS images of e) V-loaded 10% Syn-KZVI, f) V-loaded 10% Slu-KZVI.

3.7. Residual vanadium concentration test with spiked groundwater

The groundwater tests revealed that both classes of modified adsorbents were able to achieve a low residual vanadium concentration of <40 µg/l (Table 3). The impressive removal rate recorded during the residual experiment also proves the effectiveness and applicability of the modified adsorbents in the remediation of natural waters contaminated with vanadium. Detailed characterization of the treated groundwater (Table 3) revealed that the modified adsorbents were able to simultaneously remove some other pollutants, although most of the compounds and elements in the groundwater were in very low concentrations. This proves the high selectivity of the synthesized adsorbents.

Table 3. Initial and final concentration of selected ions in the spiked groundwater (SGW) after 1 g/l KZVI treatment (contact time 2 h, initial pH 6.2).

Parameter	Untreated SGW	10% Syn-KZVI treated SGW	10% Slu-KZVI treated SGW
Ammonium (mg/l)	<0.010	<0.010	<0.010
Chloride (mg/l)	12	16	9.3
Fluoride (mg/l)	<0.20	<0.20	<0.20
Nitrate (µg/l)	490	500	400
Nitrite (mg/l)	<0.011	<0.011	<0.011
Phosphate-phosphorus (µg/l)	<2.0	10	210
Sulphate (mg/l)	5.9	6.1	6.1
Aluminium (µg/l)	5.9	5.2	5.0
Barium (µg/l)	6.2	2.6	13.9
Boron (mg/l)	0.0096	8.38	18.3
Copper (µg/l)	3.2	3.4	3.6
Chromium (µg/l)	0.99	1.1	0.95
Iron (µg/l)	26.9	122	347
Manganese (µg/l)	3.3	1.6	20.5
Strontium (µg/l)	24.9	23.3	20.1
Vanadium (µg/l)	197	12.1	39.5
Zinc (µg/l)	3.0	3.0	1.8

In contrast, the concentration of some elements was also recorded to have increased from their initial concentration after being treated with the modified adsorbents. A clear example is that of boron, which was observed to have multiplied a hundredfold, especially in the groundwater treated with Slu-KZVI. The high concentration of boron in the treated groundwater could be best attributed to its leaching with water from the composite adsorbent, more specifically from the shell of the ZVI particle, according to TEM and EDS. Further washing of adsorbents with ethanol was carried out, but XPS still showed a clear B 1s peak. The presence of boron on the surface of ZVI nanoparticles has been reported earlier by Li and Zhang [38] and Nurmi et al. [39]. Further studies should solve the boron problem by optimizing the washing stage during the synthesis of the materials.

Besides boron, iron leaching from both adsorbents was observed to occur. However, the leached amount was small. The use of support materials for ZVI is known to prevent the leaching of iron into the solution [40]. In addition, the leaching of manganese from Slu-KZVI was observed to a small extent and might have originated from the dissolved sludge solution (although the XPS survey spectrum did not show a clear Mn 2p peak).

Due to the observed Fe and Mn leaching into purified water, an additional leaching test was performed at different pH values (3, 5, 9 and 10, vanadium 20 mg/l, contact time 24 h, dosage 2g/l). The leaching of iron from both classes of adsorbents was below 2 mg/l (only ~1% of Fe) with the exception of very acidic pH 3 (Fig. S7). This trend is not isolated to ZVI, as it is well known that leaching is pH-dependent and hydroxides such as hematite (α-Fe_2O_3) are known to facilitate the release of Fe under very acidic and basic conditions [41]. This is in good agreement with the TEM and XRD analysis, which indicated the presence of iron oxides/hydroxides in the composite adsorbent. The highest concentration of leached manganese from the sludge composite was recorded at pH 3 (0.2 mg/l), whereas the Mn concentration recorded at other pH values was below 0.04 mg/l.

3. Conclusions

This study demonstrated that Fe-rich groundwater treatment sludge is a viable alternative to synthetic Fe chemicals for producing a kaolin-supported ZVI. Iron can be extracted from the sludge by hydrochloric acid and then the extract can be directly used in the reduction process. XRD analysis indicated that ZVI particles were formed exclusively on the kaolin and intercalation did not occur, while XPS analysis revealed that the product from iron sludge contained some impurities (P, Ca). Therefore, although it was not as "pure" as the product from synthetic Fe chemical, it could still be considered a safe product for use in non-sensitive applications. TEM depicted an asymmetrical, quasi-spherical structure with a distinctive core and shell as the morphology of the composite adsorbent before vanadium loading. The observable disappearance of the Fe-rich core after vanadium treatment suggests the oxidative dissolution of ZVI during the reaction. Due to the dual nature of the ZVI particles, which are composed of a zerovalent shell and an oxyhydroxide outer shell, two removal mechanisms are possible. The surface complexation taking place in the shell region rich in hydroxyl groups may be the primary mechanism, whereas simultaneous V(V) reduction and Fe oxidation (redox) reactions may also occur to a lesser extent. Groundwater tests revealed that a low residual vanadium concentration could be achieved. However, significant amounts of boron were leached from the adsorbents and thus washing should be optimized in further studies. The results of the present study suggest that sludge-modified adsorbent can be utilized for the environmental remediation of vanadium from polluted waters.

Acknowledgements: This work was supported by the K.H. Renlund Foundation.

4. References

[1] WHO, Vanadium Pentoxide and Other inorganic Vanadium compounds, Concise International Chemical Assessment Document 29, World Health Organization 2001, Geneva, pp. 1-59.

[2] N. Luengo-Oroz, S. Bellomo. W. D'Alessandro, High Vanadium Concentrations in Groundwater at El Hierro (Canary Islands, Spain), 10th International Hydrogeological congress, Thessaloniki 8-10 October 2014.

[3] C.E. Fiorentino, J.D. Paoloni, M.E. Sequeira, P. Arosteguy, The presence of vanadium in groundwater of southeastern extreme the Pampean region Argentina: Relationship with other chemical elements, J. Contam. Hydrol. 93 (2007) 122−129. https://doi.org/10.1016/j.jconhyd.2007.02.001.

[4] A. Aiuppa, P. Allard, W. D'Alessandro, A. Michel, F. Parello, M. Treuil, M. Valenza, Mobility and fluxes of major, minor and trace metals during basalt weathering and groundwater transport at Mt. Etna volcano (Sicily), Geochim. Cosmochim. Acta 64(11) (2000) pp. 1827−1841. https://doi.org/10.1016/S0016-7037(00)00345-8.

[5] M.T. Wright, K. Belitz, Factors controlling the regional distribution of vanadium in groundwater, Ground Water 48 (2010) 515−525. 10.1111/j.1745-6584.2009.00666.

[6] C.L. Peacock, D.M. Sherman, Vanadium(V) adsorption onto goethite (α-FeOOH) at pH 1.5 to 12: a surface complexation model based on ab initio molecular geometries and EXAFS spectroscopy, Geochim. Cosmochim Acta 68 (2004) 1723−1733. https://doi.org/10.1016/j.gca.2003.10.018.

[7] C. Namasivayam, D. Sangeetha, Removal and recovery of vanadium(V) by adsorption onto $ZnCl_2$ activated carbon: kinetics and isotherms, Adsorption 12 (2006) 103−107. https://doi.org/10.1007/s10450-006-0373-3.

[8] T. Leiviskä, J. Matusik, B. Muir, J. Tanskanen, Vanadium removal by organo-zeolites and iron-based products from contaminated natural water. J. Clean. Prod. 167 (2017) 589−600. https://doi.org/10.1016/j.jclepro.2017.08.209.

[9] Y. Zou, X. Wang, A. Khan, P. Wang, Y. Liu, A. Alsaedi, T. Hayat, X. Wang, Environmental remediation and application of nanoscale zero-valent iron and its composites for the removal of heavy metal ions: A review, Environ. Sci. Technol. 50 (2016) 7290−7304. https://pubs.acs.org/doi/10.1021/acs.est.6b01897

[10] C. Wang, W. Zhang, Synthesizing nanoscale iron particles for rapid and complete dechlorination of TCE and PCBs, Environ. Sci. Technol. 31 (1997) 2154−2156. 10.1021/es970039c.

[11] M. Stefaniuk, P. Oleszczuk, Y.S. Ok, Review on nano zerovalent iron (nZVI): form synthesis to environmental applications, Chem. Eng. J. 287 (2016) 618−632. https://doi.org/10.1016/j.cej.2015.11.046.

[12] K. He, M. Yan, Z. Huang, G. Zeng, A. Chen, T. Huang, H. Li, X. Ren, G. Chen, Fabrication of ploydopamineekaolin supported Ag nanoparticles as effective catalyst for rapid dye decoloration, Chemosphere 219 (2019) 400−408. https://doi.org/10.1016/j. chemosphere.2018.12.012

[13] M.K. Gibbons, Md.M. Mortula, G.A. Gagnon, Phosphorus adsorption on water treatment residual solids, J. Water Supply Res. Technol. Aqua, 58 (2009) 1−10. https://doi.org/10.2166/aqua.2009.017**.**

[14] Y. Zhao, C. Wang, L.A. Wendling, Y. Pei, Feasibility of using drinking water treatment residuals as a novel chlorpyrifos adsorbent, J. Agric. Food Chem. 61 (2013) 7446−7452. 10.1021/jf401763f.

[15] B.S. Chittoo, C. Sutherland, Adsorption of phosphorus using water treatment sludge, J. Appl. Sci. 14 (2014) 3455−3463. 10.3923/jas.2014.3455.3463.

[16] Y.W. Chiang, K. Ghyselbrecht, R.M. Santos, J.A Martens, R. Swennen, V. Cappuyns, B. Meesschaert, Adsorption of multi-heavy metals onto water treatment residuals:

sorption capacities and applications, Chem. Eng. J. 200−202 (2012) 405−415. https://doi.org/10.1016/j.cej.2012.06.070.

[17] I.W. Oliver, C.D. Grant, R.S Murray, Assessing effects of aerobic and anaerobic conditions on phosphorus sorption and retention capacity of water treatment residuals. J. Environ. Manage. 92 (2011) 960−966. https://doi.org/10.1016/j.jenvman.2010.11.016.

[18] C.-H. Wang, S.-J. Gao, T.-X. Wang, B.-H. Tian, Y.-S. Pei, Effectiveness of sequential thermal and acid activation on phosphorus removal by ferric and alum water treatment residuals, Chem. Eng. J. 172 (2011) 885−891. https://doi.org/10.1016/j.cej.2011.06.078.

[19] T. Leiviskä, A. Sarpola, J. Tanskanen, Removal of lipophilic extractives from debarking wastewater by adsorption on kaolin or enhanced coagulation with chitosan and kaolin, Appl. Clay Sci. 61 (2012) 22-28. https://doi.org/10.1016/j.clay.2012.03.002.

[20] K. Rybka, K. Suwała, P. Maziarz, J. Matusik, Efficiency of Pb(II) and Mo(VI) removal by kaolinite impregnated with zero-valent iron particles, Mineralogia 48 (2017) 71−81. 10.1515/mipo-2017-0013.

[21] J. Matusik, Arsenate, orthophosphate, sulfate, and nitrate sorption equilibria and kinetics for halloysite and kaolinites with an induced positive charge, Chem. Eng. J. 246 (2014) 244−253. https://doi.org/10.1016/j.cej.2014.03.004

[22] Ç. Üzüm, T. Shahwan, A.E. Eroğlu, K.R. Hallam, T.B. Scott, I. Lieberwirth, Synthesis and characterization of kaolinite-supported zero-valent iron nanoparticles and their application for the removal of aqueous Cu^{2+} and Co^{2+} ions, Appl. Clay Sci. 43 (2009) 172−181. https://doi.org/10.1016/j.clay.2008.07.030

[23] H. Lu, J. Wang, S. Ferguson, T. Wang, Y. Bao, H. Hao, Mechanism, synthesis and modification of nano zerovalent iron in water treatment, Nanoscale 8 (2016) 9962−9975. 10.1039/C6NR00740F.

[24] Y. Xi, M. Mallavarapu, R. Naidu, Reduction and adsorption of Pb^{2+} in aqueous solution by nano-zero-valent iron—a SEM, TEM and XPS study, Mater. Res. Bull. 45 (2010) 1361−1367. https://doi.org/10.1016/j.materresbull.2010.06.046.

[25] X. Li, D.W. Elliot, W. Zhang, Zero-valent iron nanoparticles for abatement of environmental pollutants: materials and engineering aspects, Crit. Rev. Solid State Mater. Sci. 31 (2006) 111−122. http://doi/abs/10.1080/10408430601057611

[26] A.E. Yayayürük, O. Yayayürük, Adsorptive performance of nanosized zero-valent iron for V(V) removal from aqueous solutions, J. Chem. Technol. Biotech. 92 (2017) 1891−1898. https://doi.org/10.1002/jctb.5209.

[27] Q. Wang, S. Snyder, J. Kim, H. Choi, Aqueous ethanol modified nanoscale zerovalent iron in bromate reduction: synthesis, characterization, and reactivity. Environ. Sci. Technol. 43 (2009) 3292−3299. https://pubs.acs.org/doi/pdf/10.1021/es803540b

[28] C.A. Ruiz-Torres, R.F. Araujo-Martínez, G.A. Martínez-Castañón, J.E. Morales-Sánchez, T.-J. Lee, H.-S. Shin, Y. Hwang, A. Hurtado-Macías, F. Ruiz. A cost-effective method to prepare size-controlled nanoscale zero-valent iron for nitrate reduction, Environ. Eng. Res. (2019). https://doi.org/10.4491/eer.2018.320.

[29] M. Ivanić, N. Vdović, S. de Brito Barreto, V. Bermanec, I. Sondi, Mineralogy, surface properties and electrokinetic behavior of kaolin clays derived from naturally occurring pegmatite and granite deposits. Geol. Croatia 68 (2015) 139−145. https://doi.org/10.4154/GC.2015.09.

[30] S.R. Kanel, B. Manning, L. Charlet, H. Choi, Removal of arsenic-(III) from groundwater by nano scale zero-valent iron, Environ. Sci. Technol. 39 (2005) 1291−1298. 10.1021/es048991u

[31] S.R. Kanel, J.-M. Greneche, H. Choi, Arsenic(V) removal from groundwater using nano scale zero-valent iron as a colloidal reactive barrier material, Environ. Sci. Technol. 40 (2006) 2045−2050. https://pubs.acs.org/doi/abs/10.1021/es0520924.

[32] S.E. Baltazar, A. Garcia, A.H. Romero, M.A. Rubio, N. Arancibia-Miranda, D. Altbir, Surface rearrangement of nanoscale zerovalent iron: the role of pH and its implications in the kinetics of arsenate sorption, Environ. Technol. 35 (2014) 2365−2372. https://doi.org/10.1080/09593330.2014.904932

[33] S. Wang, B. Gao, Y. Li, A.E. Creamer, F. He, Adsorptive removal of arsenate from aqueous solutions by biochar supported zero-valent iron nanocomposite: Batch and continuous flow tests, J. Hazard. Mater. 322 (2017) 172−181. https://doi.org/10.1016/j.jhazmat.2016.01.052.

[34] A.M. Azzam, S.T. El-Wakeel, B.B. Mostafa, M.F. El-Shahat, Removal of Pb, Cd, Cu and Ni from aqueous solution using nano scale zero valent iron particles, J. Environ. Chem. Eng. 4 (2016) 2196−2206. https://doi.org/10.1016/j.jece.2016.03.048

[35] P. Phoempoon, L. Sikong, 2014. Phase Transformation of VO_2 nanoparticles assisted by microwave heating, Sci. World J. 841418. http://dx.doi.org/10.1155/2014/841418.

[36] M. Hadnadjev, T. Vulic, R. Marinkovic-Neducin, Y. Suchorski, H. Weiss. The iron oxidation state in Mg-Al-Fe mixed oxides derived from layered double hydroxides: An XPS study, Appl. Surf. Sci. 254 (2008) 4297−4302. https://doi.org/10.1016/j.apsusc.2008.01.063.

[37] F. Ureña-Begara, A. Crunteanu, J.P. Raskin, Raman and XPS characterization of vanadium oxide thin films with temperature. Appl. Surf. Sci. 403 (2017) 717–727. https://doi.org/10.1016/j.apsusc.2017.01.160

[38] X.-q Li, W.-x. Zhang. Sequestration of metal cations with zerovalent iron nanoparticles: A study with high resolution X-ray photoelectron spectroscopy (HR-XPS), J. Phys. Chem. C, 111 (2007) 6939−6946.

[39] J.T. Nurmi, P.G. Trantnyek, V. Sarathy, D.R. Baer, J.E. Amonette, K. Pecher, C. Wang, J.C. Linehan, D.W. Matson, R.L Penn, M.D. Driessen. Characterization and properties of metallic Iron nanoparticles: electrochemistry, environment and kinetics, Environ. Sci. Technol. 39 (5) (2005) 1221−1230.

[40] Y. Zhang, Y. Li, X. Zheng, Removal of atrazine by nanoscale zero valent iron supported on organobentonite. Sci. Total Environ. 409 (2011) 625–630. 10.1016/j.scitotenv.2010.10.015.

[41] K. Komonweeraket, B. Cetin, A.H. Aydilek, C.H. Benson, T.B. Edil. Effects of pH on the leaching mechanisms of elements from fly ash mixed soils, Fuel 140 (2015) 788−802. https://doi.org/10.1016/j.fuel.2014.09.068.